of IgE under fixed dosages.[5] However, the discrepant results of omalizumab in treating AD might be attributed to the complex immune dysregulation of AD other than IgE as the primary pathogenic mechanism. Hotze et al[8] reported that none of the patients carrying a filaggrin mutation responded to therapy, whereas all responders were nonfilaggrin mutation carriers and characterized by the presence of high concentrations of glycerophospholipids, indicating that patients with primary skin barrier deficiency were less likely to benefit from an immunomodulatory treatment with anti-IgE.

The limitations of this review included the fact that most of the existing articles were case series and the sample sizes with complete individual data were rather limited. The disease severity scoring systems also varied among the studies. Few studies provided comprehensive immunologic data that could allow systemic analysis.

There was no concrete evidence of the overall effectiveness of omalizumab for AD from this meta-analysis and systematic review based on existing small-scale case series and RCTs. Forty-three percent of the patients with AD could achieve remarkable clinical response after omalizumab treatment. Potential therapeutic benefits might be seen in selected patients with lower serum concentrations of IgE. More RCTs should be performed to clarify the potential benefits in the subgroups of patients with AD. The optimal dosage of omalizumab for patients with AD with higher IgE levels should also be further studied.

*Hsiao-Han Wang, MD*[a,b]
*Yu-Chuan Li, MD, PhD*[a]
*Yu-Chen Huang, MD*[a,b]

From [a]the Department of Dermatology, Wan Fang Hospital and [b]the Department of Dermatology, School of Medicine, College of Medicine, Taipei Medical University, Taipei, Taiwan. E-mail: dhist2002@yahoo.com.tw.

Disclosure of potential conflict of interest: The authors declare that they have no relevant conflicts of interest.

## REFERENCES

1. Makris MP, Papadavid E, Zuberbier T. The use of biologicals in cutaneous allergies—present and future. Curr Opin Allergy Clin Immunol 2014;14:409-16.
2. Krathen RA, Hsu S. Failure of omalizumab for treatment of severe adult atopic dermatitis. J Am Acad Dermatol 2005;53:338-40.
3. Lane JE, Cheyney JM, Lane TN, Kent DE, Cohen DJ. Treatment of recalcitrant atopic dermatitis with omalizumab. J Am Acad Dermatol 2006;54:68-72.
4. Vigo PG, Girgis KR, Pfuetze BL, Critchlow ME, Fisher J, Hussain I. Efficacy of anti-IgE therapy in patients with atopic dermatitis. J Am Acad Dermatol 2006; 55:168-70.
5. Sheinkopf LE, Rafi AW, Do LT, Katz RM, Klaustermeyer WB. Efficacy of omalizumab in the treatment of atopic dermatitis: a pilot study. Allergy Asthma Proc 2008;29:530-7.
6. Heil PM, Maurer D, Klein B, Hultsch T, Stingl G. Omalizumab therapy in atopic dermatitis: depletion of IgE does not improve the clinical course—a randomized, placebo-controlled and double blind pilot study. J Dtsch Dermatol Ges 2010;8: 990-8.
7. Iyengar SR, Hoyte EG, Loza A, Bonaccorso S, Chiang D, Umetsu DT, et al. Immunologic effects of omalizumab in children with severe refractory atopic dermatitis: a randomized, placebo-controlled clinical trial. Int Arch Allergy Immunol 2013; 162:89-93.
8. Hotze M, Baurecht H, Rodriguez E, Chapman-Rothe N, Ollert M, Fölster-Holst R, et al. Increased efficacy of omalizumab in atopic dermatitis patients with wild-type filaggrin status and higher serum levels of phosphatidylcholines. Allergy 2014;69:132-5.
9. Kornmann O, Watz H, Fuhr R, Krug N, Erpenbeck VJ, Kaiser G. Omalizumab in patients with allergic (IgE-mediated) asthma and IgE/bodyweight combinations above those in the initially approved dosing table. Pulm Pharmacol Ther 2014; 28:149-53.

Available online July 14, 2016.
http://dx.doi.org/10.1016/j.jaci.2016.05.038

## Variable phenotype and discrete alterations of immune phenotypes in CTP synthase 1 deficiency: Report of 2 siblings

*To the Editor:*

Loss-of-function homozygous mutations in the CTP synthase 1 (*CTPS1*) gene in humans have only recently been discovered and reveal the role of this gene in lymphocyte proliferation.[1] To date a single report including 8 individuals describes a severe clinical phenotype including early onset of severe chronic viral infections, recurrent encapsulated bacterial infections, and EBV-related B-cell non-Hodgkin lymphoma.[1]

We report 2 further sibling cases of CTSP1 deficiency identified through whole-exome sequencing (WES), further illustrating the phenotype of CTPS1 deficiency and demonstrating the value of WES for rapid diagnosis of primary immunodeficiency even for conditions whose phenotype is not well recognized.

The 2 siblings (boy, now 6 years old; girl, now 3 years old) described in this report are the only children of nonconsanguineous and healthy white parents with no personal or family history of immunodeficiency, autoimmunity, or EBV-related disorders. Both children had no dysmorphic features and normal growth.

The boy was born at term and was noted to have a significant burden of infections from early infancy. He was admitted to hospital at age 2 months with fever, lethargy, and poor feeding of unknown cause, responding rapidly to 48 hours of intravenous antibiotics. At age 7 months, he had an episode of invasive serotype 19A pneumococcal disease despite prior vaccination with the 13-valent pneumococcal conjugate vaccine (Prev(e)nar 13, Pfizer Inc, New York, NY) at age 2 and 4 months. At age 16 months, while on holiday in Turkey, he was admitted to hospital with severe tonsillitis and dehydration. At the age of 34 months, he developed an acute EBV infection with persistent viremia (see Fig E1 in this article's Online Repository at www.jacionline.org) but no features of hemophagocytic lymphohistiocytosis.

In addition to these hospital admissions, he suffered from recurrent otitis media and lower respiratory tract infections, and had moderate to severe eczema from the neonatal period. He developed chronic diarrhea of unknown etiology lasting for approximately 8 weeks when he was 3.5 years old. An upper and lower gastrointestinal endoscopic biopsy showed reactive lymphoid aggregates in the duodenum and colon without signs of active inflammation, ulceration, or infectious organisms.

The immunologic workup was largely normal (see Table E1 and the Methods section in this article's Online Repository at www.jacionline.org). However, he had only moderate responses to a 13-valent pneumococcal conjugate vaccine booster with poor persistence[2] of vaccine antibodies (Fig 1). He also showed rapid waning of antibodies against *H influenzae* type b polysaccharide and tetanus toxoid protein.

His younger sister first presented at the age of 8 months with a likely viral illness involving fever, possible meningitis (mild pleocytosis) and unresponsive episodes along with vomiting, and prolonged diarrhea. She also suffered from eczema and recurrent upper and lower respiratory tract infections from age 12 months. However, she did not have frequent ear infections, had never

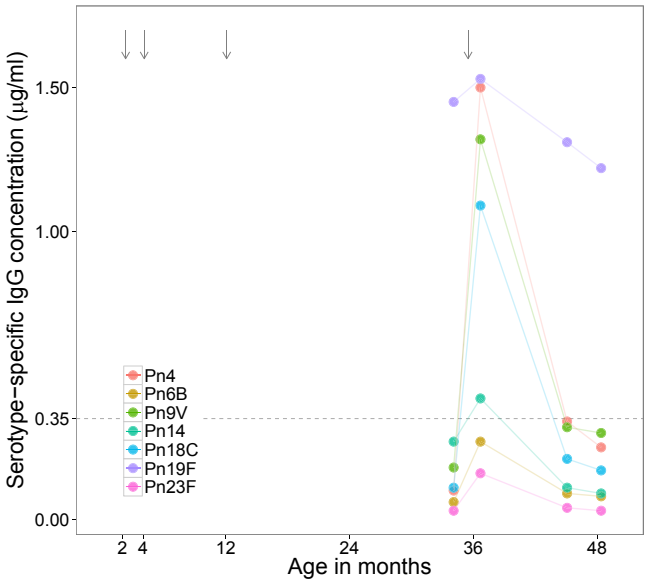


**FIG 1.** Pneumococcal serotype-specific antibody concentrations before and after booster vaccination at age 35 months. *Pn,* Pneumococcal serotype. *Arrows* indicate age at vaccination with the 13-valent pneumococcal conjugate vaccine (Prev(e)nar 13, Pfizer Inc); the *dashed line* specifies a serotype-specific IgG concentration of 0.35 μg/mL.

suffered from invasive bacterial diseases, and remains EBV negative by both PCR and serology. Initial immunological testing was normal (Table E1) apart from a poor response to a booster dose of pneumococcal conjugate vaccine and undetectable anti-*H influenzae* type b IgG concentration despite booster vaccination.

Detailed analysis of cytokine production in both children showed a normal $T_H1$ axis and normal TLR responses. However, IFN-γ production in response to T-cell agonists was significantly reduced, pointing to T-cell impairment (see Fig E2 in this article's Online Repository at www.jacionline.org).

Following negative results upon initial investigation for causes of immunodeficiency, targeted WES was performed on the affected boy when he was 4 years old. A homozygous variant within the final nucleotide in intron 17 of the *CTPS1* gene (NM_001905.2:c.1692-1G>C) was thought to be causative (see the Methods section).

Flow cytometric analysis of lymphocytes at the age of 59 and 25 months, respectively, revealed lymphopenia and marked deficiency of B cells in the boy (Fig 2, *A* and *B*), possibly resulting from chronic EBV infection (Fig E1). Both children showed a relative predominance of transitional B cells and a deficiency of naive B cells (Fig 2, *C*). The distribution of major T cells (Fig 2, *D*) and $CD4^+$ T-cell subpopulations was largely unaffected (Fig 2, *E*), whereas major disturbances were seen within the $CD8^+$ T-cell compartment (Fig 2, *F*).

The identification of the *CTPS1* mutation has significantly altered the clinical management of the 2 affected siblings, emphasizing the clinical use of next-generation sequencing in children with unknown immunodeficiencies. The index case has already successfully undergone matched unrelated donor hematopoietic stem cell transplantation (HSCT) using peripheral blood stem cells following reduced intensity conditioning with fludarabine and melphalan and *in vivo* T-cell depletion with alemtuzumab. He is now 8 months after HSCT at home and doing well without signs of graft-versus-host disease. The sister is on immunoglobulin replacement therapy and being considered for HSCT.

This report adds to the current literature by highlighting that CTPS1 deficiency can also manifest with relatively mild clinical phenotype as seen in the sister of the index case. We suggest that CTPS1 deficiency should be considered in all patients with a phenotype of combined immunodeficiency and without alternative diagnosis.[3] An important feature of CTPS1-deficient patients is that they may present with only subtle laboratory abnormalities of the humoral immune system despite experiencing severe bacterial disease. In addition, CTPS1-deficient patients can have normal immunophenotypes of major T-cell populations (Fig 2, *D*) and normal T-cell proliferation to mitogens. We found increased frequencies of transitional B cells in combination with reduced frequencies of naive B cells in both children (Fig 2, *C*). In the index patient, frequencies of naive, marginal zone, and memory B cells were greatly reduced (Fig 2, *C*), likely as a result of poor EBV control. Reduced numbers of memory B cells were also found in several patients in the original report[1] but here we show that this finding may not represent an inherent feature of CTPS1 deficiency and rather a result of chronic EBV infection. Hence, memory B-cell frequencies may be normal in CTPS1-deficient patients before EBV exposure. Within the T-cell compartment, we found reduced frequencies of activated $CD4^+$ and $CD8^+$ T cells in both patients whereas other $CD4^+$ T-cell subpopulations were present at normal frequencies. These findings are in line with results in 4 of the 8 patients described in the original report[1] who did not show lymphopenia or reduced numbers of naive $CD4^+$ T cells and therefore these recently suggested diagnostic features[4] may not be sensitive in identifying CTPS1-deficient patients. We found marked alterations of the $CD8^+$ T-cell compartment in our patients, mainly reduced frequencies of terminally differentiated and memory $CD8^+$ subpopulations (Fig 2, *F*), possibly as a result of both chronic EBV infection and the underlying defect in *CTPS1*. Taken together, CTPS1 deficiency may be suggested in children with recurrent viral and bacterial infections and reduced frequencies of activated $CD4/8^+$ T cells and abnormal $CD8^+$ phenotype with a predominance of naive $CD8^+$ T cells. Abnormalities of lymphocyte numbers, naive $CD4^+$ T-cell, and memory B-cell frequencies and the capacity of T cells to proliferate upon exposure to mitogens seem to be variable features and may also depend on previous exposure to EBV.

CTPS1 deficiency expands the range of primary immune deficiencies associated with poor EBV control and lymphoproliferation.[3] At present very little is known about the clinical phenotype or prognosis of patients with CTPS1 deficiency. Our 2 patients presented with clinical features suggestive of combined immunodeficiency and in contrast to previously described cases,[1] the clinical features also included gastrointestinal symptoms and eczema, possibly as a result of immune dysregulation. These latter features have not previously been described in CTPS1-deficient patients.

The utility of next-generation DNA sequencing in the diagnosis of rare diseases is now widely appreciated.[5] This technology offers rapid and cost-effective detection of known mutations in *PID* genes. In this report, we demonstrate that in a clinical setting where a range of genotypes may be responsible for the observed

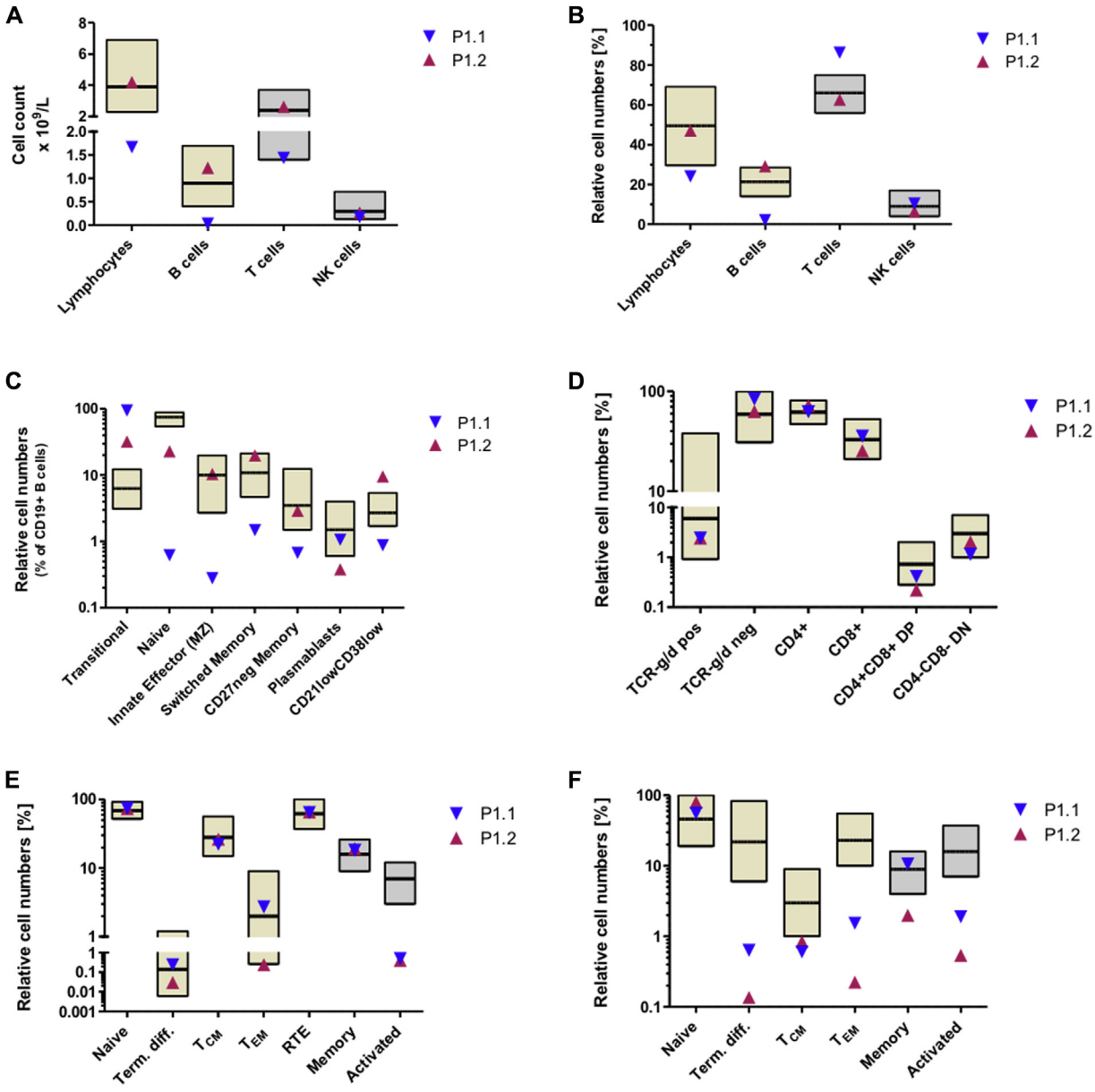


**FIG 2. A,** Absolute lymphocyte and B-, T-, and NK-cell counts. **B,** Relative lymphocyte and B-, T-, and NK-cell values. **C,** Relative numbers for B-cell subpopulations. **D,** Relative frequencies of major T-cell subsets. **E,** Relative frequencies of $CD4^+$ T-cell subpopulations. **F,** Relative frequencies of $CD8^+$ T-cell subpopulations. *DN*, Double negative; *DP*, double positive; *NK*, natural killer; $T_{CM}$, central memory T cells; $T_{EM}$, effector memory T cells; *RTE*, recent thymic emigrants.

phenotype, WES offers a novel approach in establishing a definitive diagnosis affecting the proband and other family members.

We thank the High-Throughput Genomics Group at the Wellcome Trust Centre for Human Genetics (funded by Wellcome Trust grant reference no. 090532/Z/09/Z and Medical Research Council Hub grant no. G0900747 91070) for the generation of the sequencing data.

*Johannes Trück, MD, DPhil*[a]
*Dominic F. Kelly, MRCP, PhD*[a]
*John M. Taylor, PhD*[b]
*Anne Kathrin Kienzler, PhD*[c]
*Tracy Lester, FRCPath, PhD*[b]
*Anneke Seller, FRCPath, PhD*[b]
*Andrew J. Pollard, FRCPCH, PhD*[a]
*Smita Y. Patel, FRCP, FRCPath, PhD*[c]

From [a]the Department of Paediatrics, University of Oxford, and the NIHR Oxford Biomedical Research Centre, Oxford, United Kingdom; [b]Oxford Medical Genetics Laboratories, Oxford University Hospitals NHS Trust, The Churchill Hospital, Headington, Oxford, United Kingdom; and [c]the Clinical Immunology Group, Oxford NIHR Biomedical Research Centre, United Kingdom. E-mail: johannes.trueck@kispi.uzh.ch.

This work was supported by the National Institute for Health Research (NIHR) Biomedical Research Centre Oxford with funding from the Department of Health's NIHR Biomedical Research Centres funding scheme.

Disclosure of potential conflict of interest: D. F. Kelly has received grants from the Biotechnology and Biological Sciences Research Council and GlaxoSmithKline and has received travel support from GlaxoSmithKline and Sanofi-Pasteur. S. Y. Patel

has received grants from the Wellcome Trust and has received payment for lectures from Biotest and Activis. The rest of the authors declare that they have no relevant conflicts of interest.

## REFERENCES

1. Martin E, Palmic N, Sanquer S, Lenoir C, Hauck F, Mongellaz C, et al. CTP synthase 1 deficiency in humans reveals its central role in lymphocyte proliferation. Nature 2014;510:288-92.
2. Trück J, Snape MD, Tatangeli F, Voysey M, Yu LM, Faust SN, et al. Pneumococcal serotype-specific antibodies persist through early childhood after infant immunization: Follow-up from a randomized controlled trial. PLoS One 2014;9:e91413.
3. Taylor GS, Long HM, Brooks JM, Rickinson AB, Hislop AD. The immunology of Epstein-Barr virus-induced disease. Annu Rev Immunol 2015;33:787-821.
4. Bonilla FA, Khan DA, Ballas ZK, Chinen J, Frank MM, Hsu JT, et al. Practice parameter for the diagnosis and management of primary immunodeficiency. J Allergy Clin Immunol 2015;136:1186-205, e1-78.
5. Casanova J-L, Conley ME, Seligman SJ, Abel L, Notarangelo LD. Guidelines for genetic studies in single patients: lessons from primary immunodeficiencies. J Exp Med 2014;211:2137-49.

Available online July 14, 2016.
http://dx.doi.org/10.1016/j.jaci.2016.04.059

## Platelet-activating factor decreases skin keratinocyte tight junction barrier integrity

*To the Editor:*

Keratinocytes (KCs) build the epidermis, an efficient barrier that prevents microbial pathogens and environmental agents including allergens from entering into the skin.[1] Pathological changes in skin KCs are commonly associated with many skin diseases, such as atopic dermatitis (AD), urticaria, and psoriasis. It was recently reported in the *Journal of Allergy and Clinical Immunology* that there are tight junction (TJ) defects that lead to a disruption of epithelial barrier function of KCs in the skin of patients with AD[2] and in the meantime evidence for the genetic and immune regulatory mechanisms that control TJ defects has been reported.[1,3,4] Barrier-related molecules in the epidermis are regulated by inflammatory responses derived from both the epidermal (ie, KCs and Langerhans cells) and immune cells (ie, T cells, dendritic cells, and other cells). Platelet-activating factor (PAF) is an important proinflammatory factor produced and secreted by several types of cells, including mast cells, monocytes, tissue macrophages, platelets, eosinophils, endothelial cells, and neutrophils, and is involved in allergic inflammation.[5] In this letter, we emphasize the influence of PAF on skin barrier and KC TJ integrity in AD and further analyze TJ disruption in diseased skin for better understanding the molecular and cellular mechanisms in the regulation of TJ barrier integrity.

First, we investigated the role of PAF in the regulation of TJ function of human KCs. Normal human skin KCs from healthy subjects and skin KCs from patients with AD were cultured at air-liquid interface (ALI) and transepithelial resistance (TER) was measured as a readout for barrier integrity. Two days after reaching maximal TER, ALI cultures were stimulated with different concentrations of PAF and TER was measured before and 24, 48, 72, and 96 hours after stimulation. In resting conditions without any stimulation, TER levels in AD KCs were significantly lower than in healthy KCs (Fig 1, *A*). PAF decreased the TER starting from 48 hours and after stimulation of ALI cultures of human KCs. Although AD KCs seem to show a relatively late response to PAF compared with healthy KCs in the early time points such as 24 and 48 hours, there was no difference in percent increase after 72 and 96 hours (Fig 1, *B*). Notably, changes in TER are taking place relatively late, becoming significant after 48 hours. A part of this effect can be due to secondary mediators, such as cytokines that modify TJ integrity. It has been reported that PAF activates epithelial cells to release several cytokines and several cytokines have been reported to regulate TJs.[5] In accordance with this, we observed an increase in paracellular flux of fluorescein isothiocyanate–labeled dextran 4 kDa in response to PAF treatment, indicating a comparable decrease in TJ barrier integrity in both groups (Fig 1, *C*).

Upon binding to the PAF receptor, PAF activates downstream signaling pathways leading to increased intracellular $Ca^{2+}$ flux.[6] To investigate the downstream regulation of PAF on TJ, we stimulated KCs of healthy individuals and KCs of individuals with AD with ionomycin, an agonist inducing intracellular $Ca^{2+}$ flux, and found that ionomycin rapidly decreased TER (Fig 1, *D*). The present study strongly suggests that the influence of PAF on barrier function is controlled by the induction of intracellular $Ca^{2+}$ influx, because induction of $Ca^{2+}$ flux alone with $Ca^{2+}$ ionophore in the epithelium disrupts TJ barrier integrity. This finding does not exclude other signaling events via the PAF receptor, and has implications on other molecules working on the same family of G-protein coupled receptors that are inducing $Ca^{2+}$ flux. As repeatedly reported in other cells, we also observed that the leakiness of AD KCs stays stable after many passages. We agree that there might be many reasons for this finding including prolonged exposure to $T_H2$ environment starting early in life. It is practically not possible that these epigenetic changes are the same in every individual, so variation between donors can be observed.

To investigate TJ barrier directly in the context of human skin diseases, we analyzed mRNA expression and TJ protein integrity in skin biopsies. Immunofluorescence staining of occludin and claudin-7 showed an intact TJ layer in healthy skin (Fig 2, *A* and *B*). TJ integrity was disrupted in AD skin, more severely in lesional AD than in nonlesional AD skin, manifesting with a patchy, disrupted, and less dense arrangement of protein expression of TJs (Fig 2, *B*). A full disruption of TJs expression was observed in some parts of AD lesions. Skin prick tests induce immediate allergic reaction and urticaria is another PAF-associated skin disease. As an important finding that may open a new window for future research, the TJ layer integrity was decreased in skin prick tests and urticaria in comparison to healthy skin (Fig 2, *A*).

We then further analyzed whether the defects in protein expression of TJs were due to a transcriptional regulation that affects mRNA levels. We used a low-density array microfluidic card (Applied Biosystems, Carlsbad, Calif), which contains all known junctional and junction-associated proteins that are expressed in the epidermis and epithelia.[7] In addition to TJ proteins, desmosomes, gap junctions, adherens junctions, and adaptor protein genes were included in the analysis. We observed decreased mRNA expression of claudin-7 in skin prick test biopsies, and decreased mRNA expressions of claudin-3, claudin-7, claudin-8, claudin-14, and occludin in urticaria biopsies compared with healthy skin biopsies (see Fig E1 in this article's Online Repository at www.jacionline.org). Similarly, the mRNA expressions of occludin, claudin-7, claudin-2, claudin-8, claudin-12, claudin-23, as well as several other

# METHODS

## Additional immune workup in the index case

In addition to the analysis presented in Table E1, normal results were found for T-cell receptor V-beta repertoire, T-cell-receptor gene rearrangement excisional circles, CD62 ligand shedding, SLAM-associated protein and X-linked inhibitor of apoptosis protein protein expression, and IL-2–inducible T-cell kinase expression and genetic analysis.

## Whole-exome sequencing

This was done as part of a research project approved by the Southampton A Research Ethics Committee (reference 12/SC/044), and written informed consent was obtained from both parents.

Exome capture was performed using the NimbleGen SeqCap EZ Human Exome Library v2.0, according to the manufacturer's instructions, and sequenced using a 2 × 100 bp read protocol on an Illumina HiSeq. Approximately 15 Gb of sequence was obtained, providing at least 10 × vertical read depth over approximately 90% of the coding exome, as specified by the consensus coding sequence project. Reads were aligned to hg19 with Stampy (v1.0.20)[E1] and variant calling of single nucleotide variants and short insertion and deletions was undertaken using Platypus (v0.5.2; www.well.ox.ac.uk/platypus).[E2]

Variant annotation and analysis was restricted to a targeted panel of 237 immune-related genes (Table E2), using the Illumina VariantStudio data analysis software (Illumina, Inc, San Diego, Calif). Variants were initially filtered on a population frequency below 5% within the National Heart, Lung, and Blood Institute GO Exome Sequencing Project,[E3] which reduced the list from 284 variants to 44 variant calls. All variants were individually assessed to determine their likely pathogenicity on the basis of ACGS-recommended best practice guidelines.[E4]

Subsequent Sanger sequencing demonstrated that this homozygous nucleotide substitution was present in both affected children and heterozygous in both unaffected parents. This change has recently been described in several affected members of families originating from the northwest of England[E5] and disrupts 1 of the 2 invariant nucleotides of the acceptor site and is predicted to lead to aberrant splicing of intron 17 (Alamut, version 2.4.5; Interactive Biosoftware, Rouen, France) (Fig E3). It is therefore considered to be pathogenic.

## Immune phenotyping by flow cytometry

Absolute lymphocyte counts were determined using the BD Multitest, CD3/CD16:56/CD45/CD19 reagent, and TruCount tubes (both BD Biosciences, San Jose, Calif) according to the manufacturer's instructions. Flow cytometry data were analyzed with Infinicyt software (Cytognos, Spain). Boxplots indicate the 5 to 95th percentile and median adopted from Piątosa et al[E6] (for lymphocytes, B cells, and B-cell subpopulations), the 10 to 90th percentile and median adopted from Shearer et al[E7] (for T and natural killer [NK] cells, memory and activated CD4/8$^+$ T-cell subpopulations), and the mean and 90% tolerance interval adopted from Schatorjé et al[E8] (for major T-cell populations and most CD4/8$^+$ T-cell subpopulations). Note that gating strategies for cell populations may differ between cited reports and our report.

Additional notes with regard to the analysis of panels shown in Fig 2: **A,** Absolute numbers of lymphocytes (CD45$^+$ and scatter characteristics) and B (CD45$^+$CD19$^+$), T (CD45$^+$CD3$^+$), and NK (CD45$^+$CD16$^+$CD56$^+$) cells. **B,** Relative lymphocyte and B, T, and NK-cell values as indicated by the percentage of total CD45$^+$ leukocytes (lymphocytes) or CD45$^+$ lymphocytes (B, T, and NK cells). **C,** Relative numbers for B-cell subpopulations expressed as a percentage of total CD19$^+$ B cells: transitional B cells (CD27$^-$IgD$^+$IgM$^+$CD24$^+$CD38$^+$); naive B cells (CD27$^-$IgD$^+$IgM$^+$); innate effector/marginal zone B cells (CD27$^+$IgD$^+$IgM$^+$); switched memory B cells (CD27$^+$IgD$^-$IgM$^-$); CD27-negative memory B cells (CD27$^-$IgD$^-$IgM$^-$); plasmablasts (CD27$^+$CD38$^+$CD24$^-$); CD21low CD38low activated B cells (CD21$^{lo}$CD38$^{lo}$). **D,** Relative frequencies of major T-cell subsets: TCR-g/d positive cells (CD45$^+$TCRg/d$^+$), TCR-g/d negative cells (CD45$^+$TCRg/d$^-$), CD4$^+$T cells (TCRg/d-CD4$^+$), CD8$^+$ T cells (TCRg/d$^-$CD8$^+$), CD4$^+$CD8$^+$ double-positive T cells (TCRg/d-CD4$^+$CD8$^+$), and CD4$^-$CD8$^-$ double-negative T cells (TCRg/d$^-$CD4$^-$CD8$^-$). Relative cell counts for TCRgd-positive and TCRgd-negative T cells indicate the percentage of total CD45$^+$ lymphocytes. Relative cell counts for CD4$^+$, CD8$^+$, double-positive, and double-negative T cells depict the percentage of CD3$^+$TCRgd$^-$ T cells. **E,** Relative frequencies of CD4$^+$ T-cell subpopulations: Naive T cells (CD45RA$^+$CD27$^+$), terminally differentiated T cells (term. diff.; CD45RA$^+$CD27$^-$), central memory T cells ($T_{CM}$; CD45RA$^-$CD27$^+$), effector memory T cells ($T_{EM}$; CD45RA$^-$CD27$^-$), recent thymic emigrants (CD45RO$^-$CD31$^+$CD62L$^+$HLA$^-$DR$^-$), memory T cells (CD45RO$^+$), and activated T cells (HLA$^-$DR$^+$). Relative cell counts for CD4$^+$ naive, term. diff., $T_{CM}$, and $T_{EM}$ T cells depict the percentage of total CD4$^+$ lymphocytes. Relative cell counts for CD4$^+$ memory and activated T cells depict the percentage of CD3$^+$ T cells. **F,** Relative frequencies of CD8$^+$ T-cell subpopulations: Naive T cells (CD45RO$^-$CD27$^+$CCR7$^+$), term. diff T cells (CD45RO$^-$CD27$^-$CCR7$^-$), $T_{CM}$ (CD45RO$^+$CD27$^+$CCR7$^+$), $T_{EM}$ (CD45RO$^+$CD27$^-$CCR7$^-$), memory T cells (CD45RO$^+$), and activated T cells (HLA-DR$^+$). Relative cell counts for naive, term. diff, $T_{CM}$, and $T_{EM}$ T cells depict the percentage of total CD8$^+$ lymphocytes. Relative cell counts for memory and activated T cells depict the percentage of CD3$^+$ T cells.

## REFERENCES

E1. Lunter G, Goodson M. Stampy: a statistical algorithm for sensitive and fast mapping of Illumina sequence reads. Genome Res 2011;21:936-9.

E2. Rimmer A, Phan H, Mathieson I, Iqbal Z, Twigg SRF, Wilkie AOM, et al. Integrating mapping-, assembly- and haplotype-based approaches for calling variants in clinical sequencing applications. Nat Genet 2014;46:912-8.

E3. Available at: www.evs.gs.washington.edu/EVS/.

E4. Wallis Y, Payne S, McAnulty C, Bodmer D, Sistermans E, Robertson K, et al. Practice Guidelines for the Evaluation of Pathogenicity and the Reporting of Sequence Variants in Clinical Molecular Genetics. Available at: http://www.acgs.uk.com/committees/quality-committee/best-practice-guidelines/.

E5. Martin E, Palmic N, Sanquer S, Lenoir C, Hauck F, Mongellaz C, et al. CTP synthase 1 deficiency in humans reveals its central role in lymphocyte proliferation. Nature 2014;510:288-92.

E6. Piątosa B, Wolska-Kuśnierz B, Pac M, Siewiera K, Gałkowska E, Bernatowska E. B cell subsets in healthy children: reference values for evaluation of B cell maturation process in peripheral blood. Cytometry B Clin Cytom 2010;78B:372-81.

E7. Shearer WT, Rosenblatt HM, Gelman RS, Oymopito R, Plaeger S, Stiehm ER, et al. Lymphocyte subsets in healthy children from birth through 18 years of age: the pediatric AIDS clinical trials group P1009 study. J Allergy Clin Immunol 2003;112:973-80.

E8. Schatorjé EJH, Gemen EFA, Driessen GJA, Leuvenink J, van Hout RWNM, de Vries E. Paediatric reference values for the peripheral T cell compartment. Scand J Immunol 2012;75:436-44.

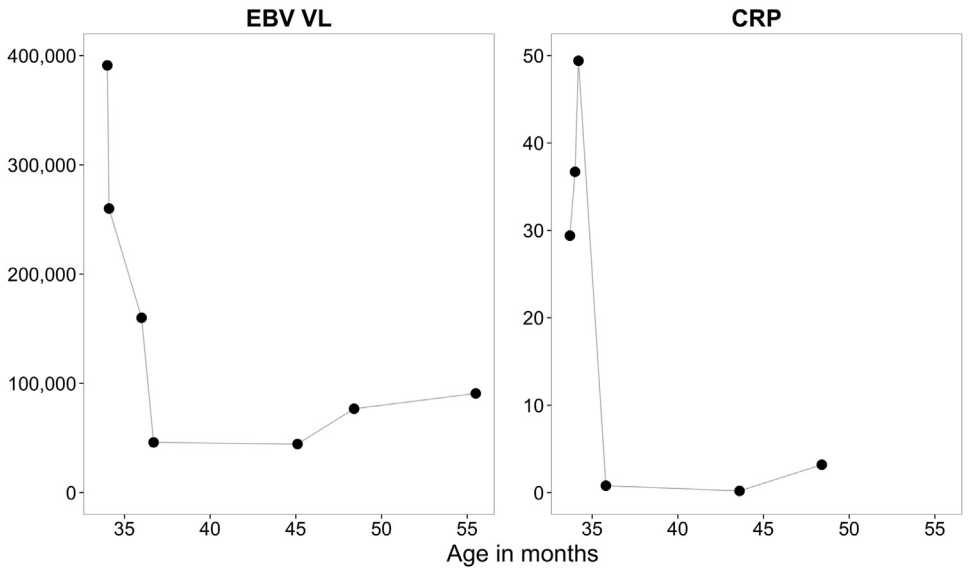


**FIG E1.** Kinetics of EBV viral load (VL [copies/mL]) and CRP (mg/L) of patient Pat_1.1 during and after the acute EBV infection at around age 34 months.

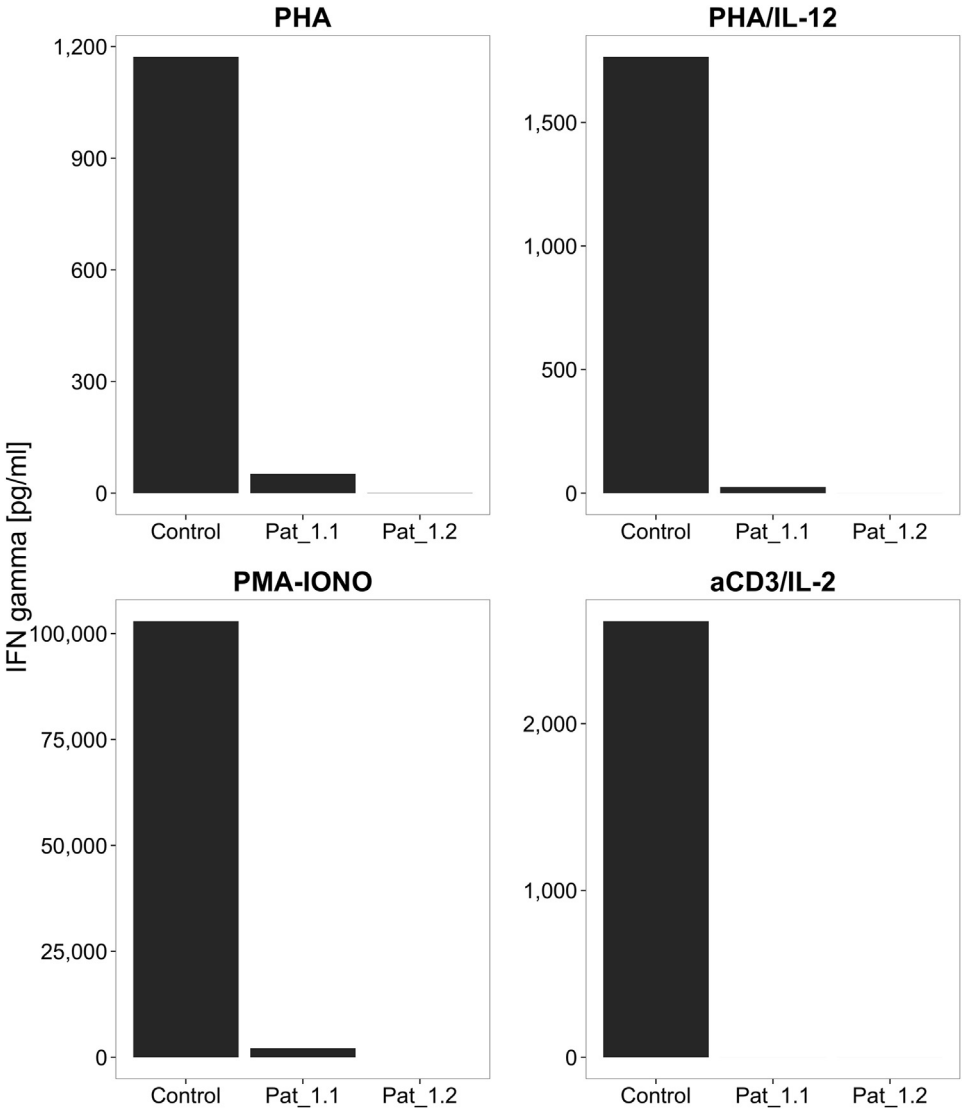


**FIG E2.** Cytokine studies on both patients (boy, Pat_1.1, and girl, Pat_1.2) and a control. Stimulating agents are shown above each bar graph, and bars show IFN-γ responses to stimulation as bars for both patients in comparison with a healthy control. *IONO*, Ionomycin; *PMA*, phorbol 12-myristate 13-acetate.

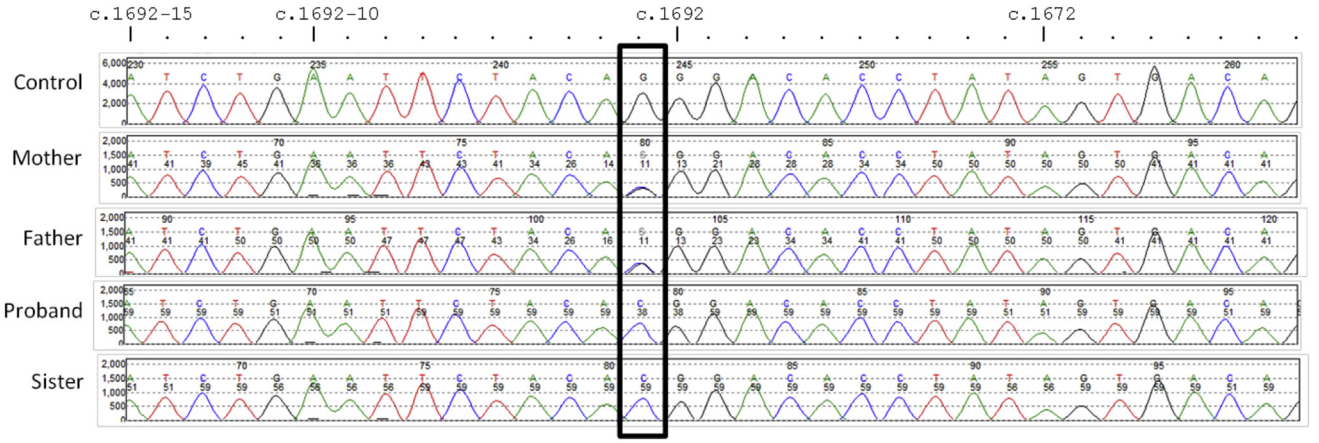


**FIG E3.** *CTPS1* sequence electropherograms for the 4 members of the kindred with the c.1692-1G >C variant (outlined by the *black box*).

**TABLE E1.** Results of immunologic investigations performed in the 2 siblings

| Patient | P1.1 (male) | P1.2 (female) |
|---|---|---|
| Age at evaluation (mo) | 42 | 9 |
| Cell subsets (cells/$mm^3$) | | |
| ANC (1.5-8.0) | 5.15 | 2.4 |
| Lymphocytes | 2.23 (1.8-5.4) | 3.11 (2.6-10.4) |
| $CD3^+$ (normal) | 1.81 (1.2-3.4) | 1.99 (1.6-6.7) |
| $CD4^+$ (normal) | 1.1 (0.8-2.1) | 1.45 (1.0-4.6) |
| $CD8^+$ (normal) | 0.62 (0.35-1.7) | 0.5 (0.4-2.1) |
| $CD19^+$ (normal) | 0.25 (0.1-0.5) | 0.89 (0.6-2.7) |
| $CD56^+$ (normal) | 0.15 (0.1-1.0) | 0.2 (0.2-1.2) |
| T-cell proliferation by CFSE (using PHA) | Normal | ND |
| Serum immunoglobulins | | |
| IgA (normal) (g/L) | 1.01 (0.4-2.0) | **0.72 (0.2-0.7)** |
| IgG (normal) (g/L) | 5.34 (4.9-13.0) | 5.58 (3.0-10.9) |
| IgM (normal) (g/L) | 0.62 (0.4-2.5) | 0.44 (0.4-2.0) |
| IgE (normal) (kU/L) | 6.49 (5-63) | ND |

Values in boldface correspond to values outside normal age-matched ranges that are indicated in parentheses.

*ANC*, Absolute neutrophil count; *CFSE*, carboxyfluorescein succinimidyl ester; *ND*, not done.

**TABLE E2.** List of targeted panel of 237 immune-related genes

| | | | | |
|---|---|---|---|---|
| *ACP5* | *CD8A* | *IL10* | *NHP2* | *SPINK5* |
| *ACTB* | *CEBPE* | *IL10RA* | *NKX2-5* | *STAT1* |
| *ADA* | *CFB* | *IL10RB* | *NLRP12* | *STAT2* |
| *ADAM17* | *CFD* | *IL12 B* | *NLRP3* | *STAT3* |
| *ADAR* | *CFH* | *IL12RB1* | *NOD2* | *STAT5B* |
| *AICDA* | *CFHR1* | *IL17F* | *NOP10* | *STIM1* |
| *AIRE* | *CFHR2* | *IL17RA* | *NRAS* | *STK4* |
| *AK2* | *CFHR3* | *IL1RN* | *ORAI1* | *STX11* |
| *AP3B1* | *CFHR4* | *IL21R* | *PIGA* | *STXBP2* |
| *APOL1* | *CFHR5* | *IL2RA* | *PIK3CD* | *TAP1* |
| *ATM* | *CFI* | *IL2RG* | *PIK3R1* | *TAP2* |
| *BLM* | *CFP* | *IL36RN* | *PLCG2* | *TAPBP* |
| *BLNK* | *CHD7* | *IL7R* | *PMS2* | *TAZ* |
| *BLOC1S6* | *CIITA* | *IRAK4* | *PNP* | *TBK1* |
| *BTK* | *COLEC11* | *IRF8* | *POLE* | *TBX1* |
| *C1QA* | *CORO1A* | *ISG15* | *PRF1* | *TCF3* |
| *C1QB* | *CR2* | *ITCH* | *PRKCD* | *TCN2* |
| *C1QC* | *CSF2RA* | *ITGB2* | *PRKDC* | *TERT* |
| *C1R* | *CTPS1* | *ITK* | *PSMB8* | *THBD* |
| *C1S* | *CTSC* | *JAK3* | *PSTPIP1* | *TICAM1* |
| *C2* | *CXCR4* | *KMT2D* | *PTPRC* | *TINF2* |
| *C3* | *CYBA* | *KRAS* | *RAB27A* | *TLR3* |
| *C4A* | *CYBB* | *LAMTOR2* | *RAC2* | *TMC6* |
| *C4B* | *DCLRE1C* | *LCK* | *RAG1* | *TMC8* |
| *C5* | *DKC1* | *LIG4* | *RAG2* | *TNFRSF13B* |
| *C6* | *DNMT3B* | *LPIN2* | *RBCK1* | *TNFRSF13C* |
| *C7* | *DOCK8* | *LRBA* | *RFX5* | *TNFRSF1A* |
| *C8A* | *ELANE* | *LYST* | *RFXANK* | *TNFRSF4* |
| *C8B* | *FADD* | *MAGT1* | *RFXAP* | *TNFSF12* |
| *C9* | *FAS* | *MALT1* | *RHOH* | *TRAF3* |
| *CARD11* | *FASLG* | *MASP1* | *RNASEH2A* | *TRAF3IP2* |
| *CARD14* | *FCN3* | *MASP2* | *RNASEH2B* | *TREX1* |
| *CARD9* | *FERMT3* | *MBL2* | *RNASEH2C* | *TTC7A* |
| *CASP10* | *FOXN1* | *MCM4* | *RNF168* | *TYK2* |
| *CASP8* | *FOXP3* | *MEFV* | *RPSA* | *UNC119* |
| *CD19* | *FPR1* | *MRE11A* | *RTEL1* | *UNC13D* |
| *CD247* | *G6PC3* | *MS4A1* | *SAMHD1* | *UNC93B1* |
| *CD27* | *G6PD* | *MSH5* | *SBDS* | *UNG* |
| *CD3D* | *GATA2* | *MTHFD1* | *SEMA3E* | *USB1* |
| *CD3E* | *GFI1* | *MVK* | *SERPING1* | *VPS13B* |
| *CD3G* | *HAX1* | *MYD88* | *SH2D1A* | *VPS45* |
| *CD40* | *ICOS* | *NBN* | *SH3BP2* | *WAS* |
| *CD40LG* | *IFNGR1* | *NCF1* | *SLC29A3* | *WIPF1* |
| *CD46* | *IFNGR2* | *NCF2* | *SLC35C1* | *XIAP* |
| *CD59* | *IGLL1* | *NCF4* | *SLC37A4* | *ZAP70* |
| *CD79A* | *IKBKB* | *NFKB2* | *SLC46A1* | *ZBTB24* |
| *CD79B* | *IKBKG* | *NFKBIA* | *SMARCAL1* | |
| *CD81* | *IKZF1* | *NHEJ1* | *SP110* | |